Department of Physics and Astronomy

UCL

High Mass $pp \rightarrow \tau\tau$ analysis

Measurement of fiducial differential $\tau^+\tau^-$ cross sections.

https://arxiv.org/pdf/2503.19836

Peng Wang

IoP Conference 2025

ATLAS EXPERIMENT

Motivation

- It is the first 13TeV measurement of the inclusive $\tau\bar{\tau}$ fiducial cross-section as a function of the invariant mass.
- Di-tau mass spectrum is sensitive to new physics that has enhanced couplings to 3rd generation fermions.
- New Physics is expected to be in the high mass region, allowing Effective Field Theory (EFT) interpretation.

SM Drell-Yan $\tau\tau$

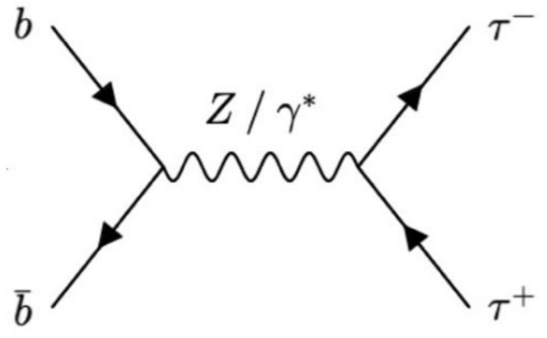

	Opposite-Sign	Same-Sign
$\tau_{had}\tau_{had}$	Measurement Inclusive in b-jet multiplicity.	Fake Tau Background Validation Region
$e\tau_{had}$ $\mu\tau_{had}$	VV and ttbar Validation Region	

Standard ATLAS algorithms and calibrations are used for physics object reconstruction.

Analysis Strategy

- Using Full Run 2 13TeV pp dataset (140/fb).
- High mass region $m_{\tau\tau}^{vis} > 100\ \text{GeV}$
- Channels are split into:
  - **Fully hadronic** ($\tau_{had}\tau_{had}$, signal) and **Semi-leptonic** ($e\tau_{had}$ and $\mu\tau_{had}$, validation)
  - **Opposite-sign** (signal) and **same-sign** (validation)
- Drell-Yan purity is lower when there is one or more leptonic decays.
- Measurement inclusive in b-jet multiplicity, whereas the parallel search split into b-jet multiplicity bins.
- **Any event that meets the particle-level fiducial requirements is treated as signal regardless of their production process**

Fake Estimate

Fake-tau backgrounds are estimated using the data-driven **Universal Fake Factors (FF) method:**

- A Recurrent Neural Network (RNN) identification algorithm is used to separate out fake taus.
- RNN>0.8 for τ_{had} (SR ID) and we define an anti-ID region with RNN<0.8.
- The anti-ID to ID transfer factor (Fake Factor) is evaluated for three cases:
  - Quark-enriched jets ($Z \to \mu\mu$ + jet);
  - Gluon-enriched jets (multijet)
  - Pileup-enriched jets (multijet).

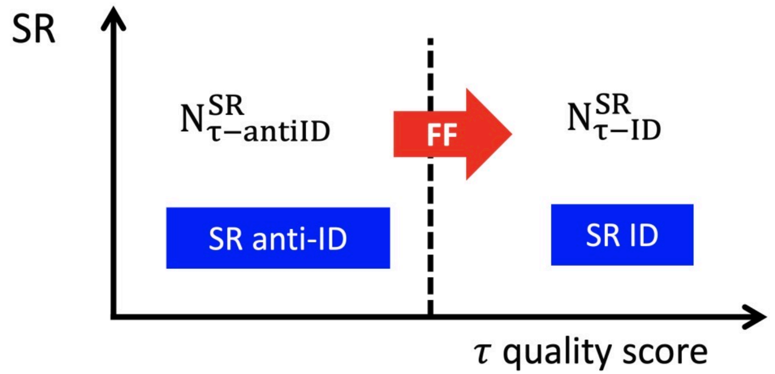

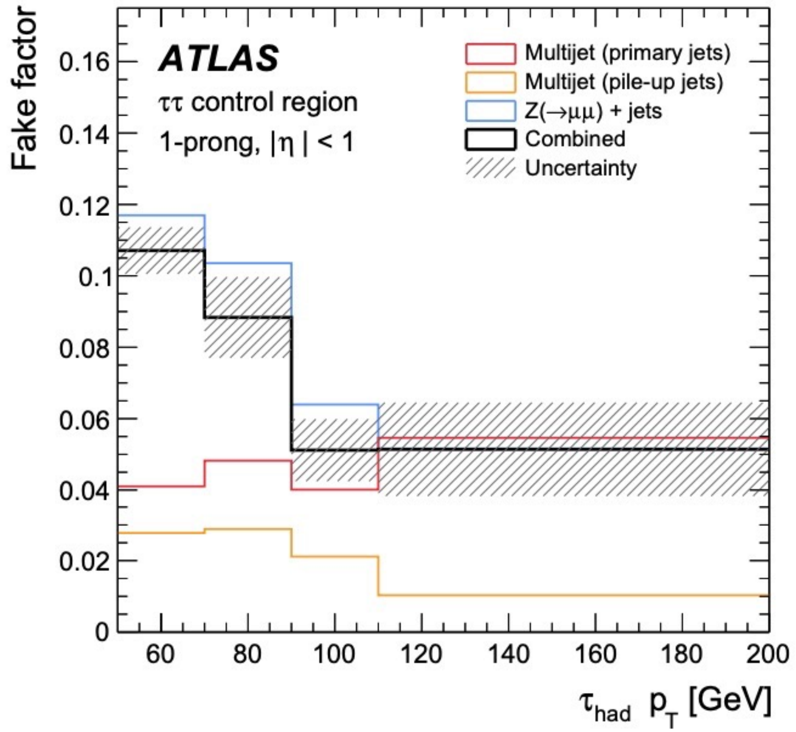

The fake factor as a function of τ_{had} p_{T} for each category of events and τ_{had} objects with one associated charged track and $|\eta| < 1$

Fakes Estimate

- Fractions of quark/gluon/pileup jets in anti-ID regions are found by fitting the τ width with ATLAS centrally provided templates.

- The FFs are combined linearly based on the template fit result:

$$FF_{comb} = \alpha_q FF_q + \alpha_g FF_{gluon} + (1 - \alpha_q - \alpha_g) FF_{pileup}$$

$\alpha_{q,g}$ are fit parameters

- The Combined FF is used to give fakes estimate.

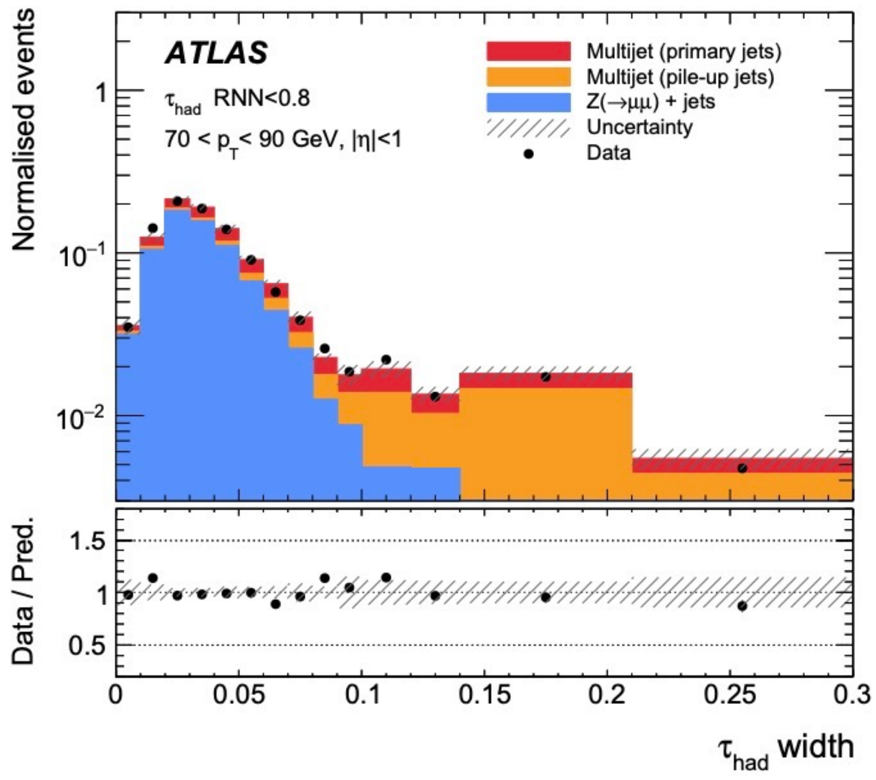

The result of the width fit for τ_{had} objects with one associated charged track, pT between 70 and 90 GeV, and $|\eta|$ < 1

Fakes Estimate Validation

- Fakes estimate is validated in the validation regions (as shown in Slide 2)
- Good SM and data agreement in same-sign $\tau_{had}\tau_{had}$ (Left) and same-sign $l\tau_{had}$ (Right) channels.

Fake tau = Misreconstructed τ_{had}

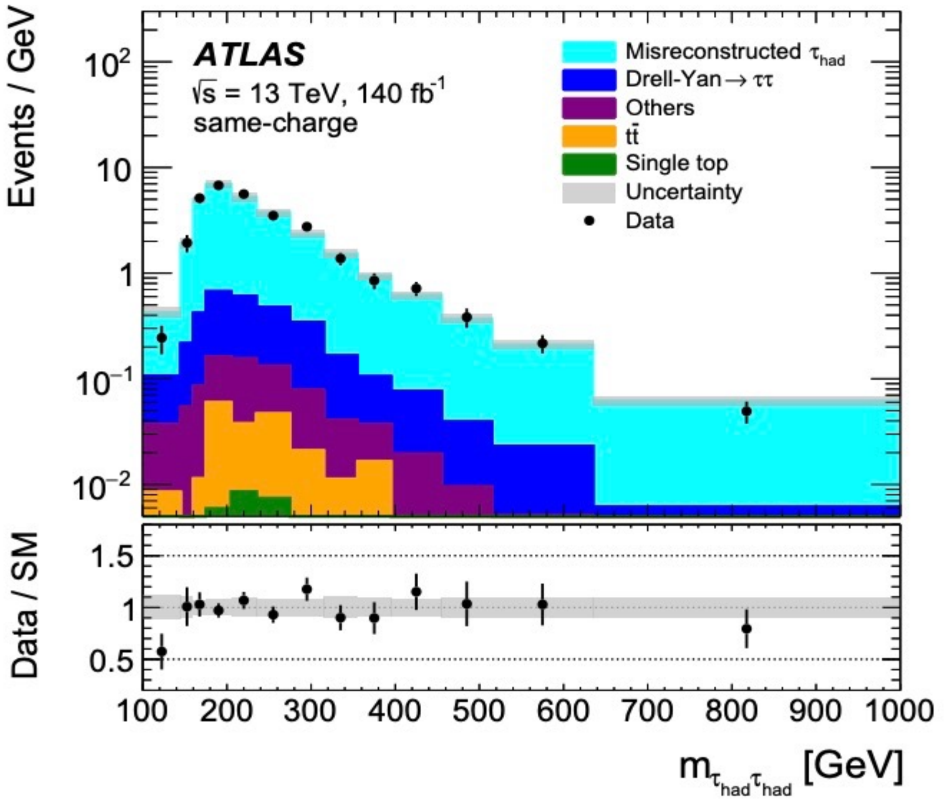

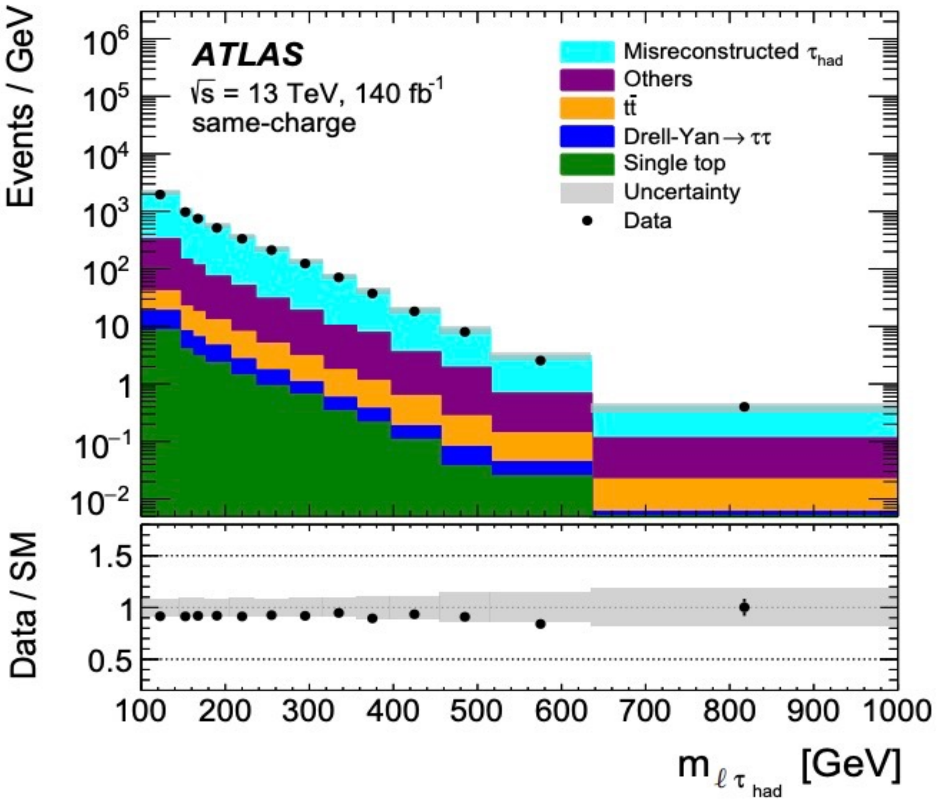

Unfolding

- **Unfolding is a process that corrects detector effects to get us to the particle-level distribution**

- **Fiducial Selection for $m_{vis}^{\tau\tau}$ distribution:** Two Opposite-Sign τ_{had} , $|\eta|$< 2.47 and leading tau p_T> 90 GeV, sub-leading tau p_T > 60GeV.

(Any event that meets the particle-level fiducial requirements is treated as signal regardless of their production process)

- Detector effects are unfolded using the [Iterative Bayesian Unfolding (IBU)]() method with 2 iterations.

- Binning is optimized to have purity (the fraction of fiducial events in the same bin for both detector-level and particle-level) greater than 0.65 everywhere.

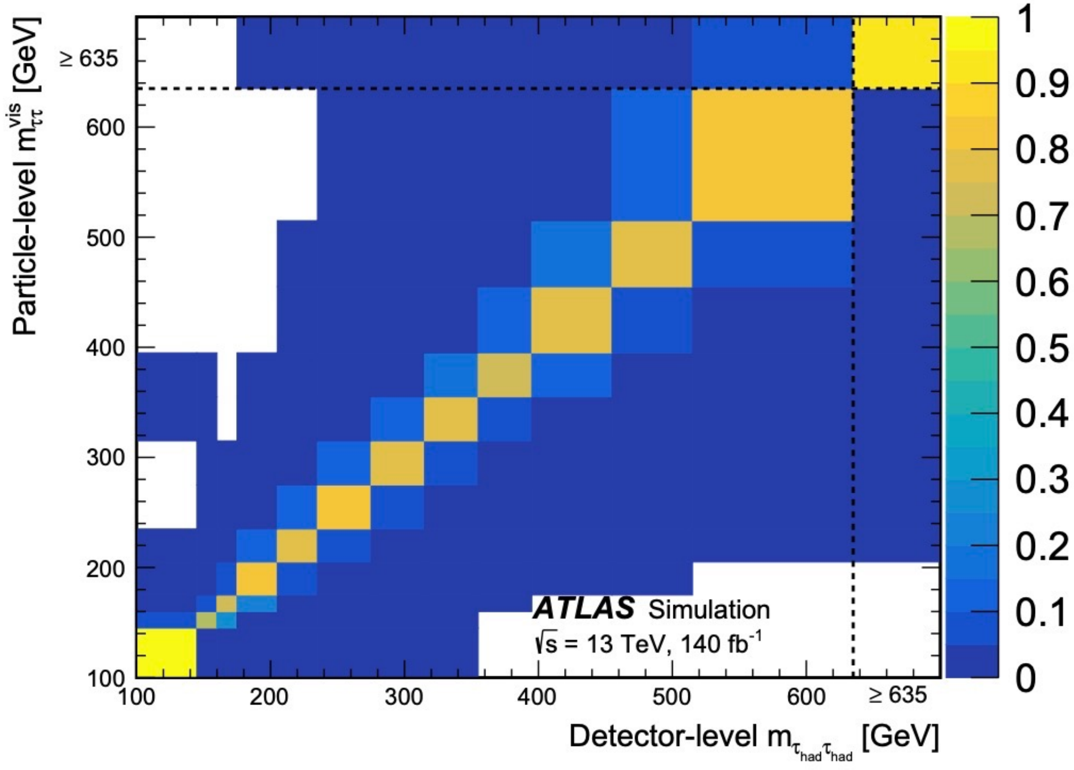

Response Matrix: migration between mass bins for fiducial events that also pass detector-level selection.

Uncertainties

Uncertainties on unfolded data

- Modelling and τ identification uncertainties dominate in most bins.
- Statistical uncertainty rises to around 15% at high-mass bins.
- High uncertainty (~50%) at low masses primarily due to the τ trigger p_T threshold.

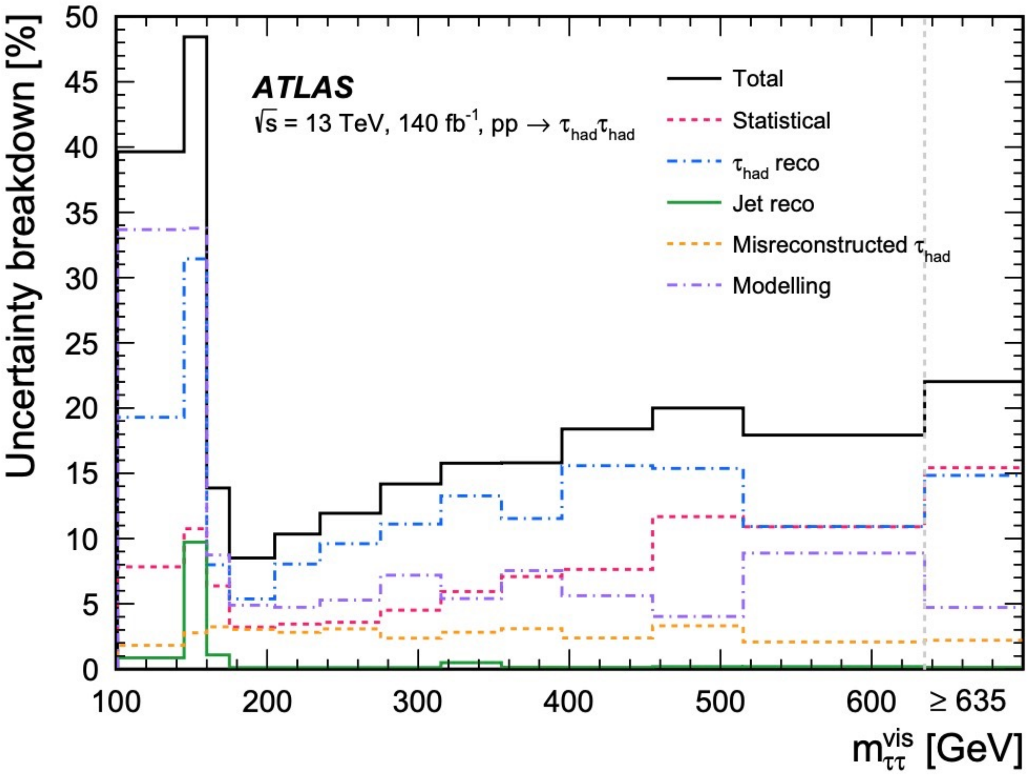

Uncertainty breakdown for the $m_{\tau\tau}^{vis}$ differential cross-section measurement.

Uncertainties

Uncertainties on SM Predictions

SM Predictions: Samples generated using Sherpa 2.2.11, Powheg+Pythia8

- **Scale Uncertainties**: Envelope of 7-point variation
  - Variation in Renormalisation and Factorization parameters by a factor of 2

- **PDF Uncertainties**: Calculated using LHAPDF Tool
  - Hessian eigenvector set from **NNPDF3.0nnlo** was used for samples generated with Sherpa 2.2.11.
  - Replica set from **NNPDF3.0nlo** was used for samples generated with Powheg+Pythia8.

Unfolding

unblinded data compared with SM Predicitons

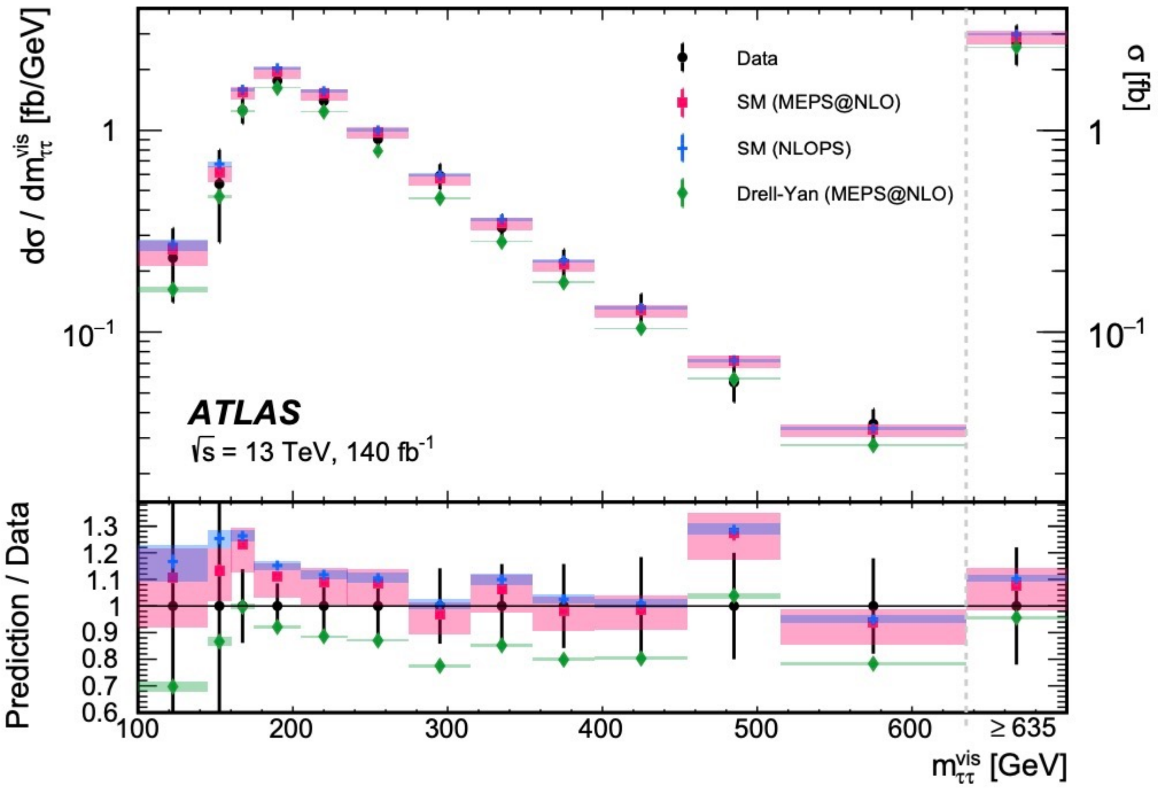

- **Data**: Unfolded data points, error bars include experimental + modelling + statistical uncertainties.
- MC prediction error bars include QCD scale and PDF uncertainties.
- Under the assumption that theory and experimental uncertainties are normally distributed, **fitting MEPS@NLO SM prediction with unfolded data gives a p-value of 0.78.**
- **Drell-Yan MEPS@NLO** includes only Statistical uncertainties, this is only to demonstrate the Drell-Yan process contribution to the entire stack.

Interpretation

SM Effective Field Theory (SMEFT)

- General Lagrangrian of an EFT respecting the Standard Model gauge symmetries:

$$\mathcal{L}_{\text{SMEFT}} = \mathcal{L}_{\text{SM}} + \sum_i \frac{c_i O_i^{(6)}}{\Lambda^2} + \dots,$$

  - ➢ With coupling coefficients c_i, dimension 6 operators $O_i^{(6)}$ and suppression mass scale Λ.
- Relevant coupling coefficients to this analysis: four-fermion operators.
- Using the 'top' model, which assumes flavour-symmetry for the first two quark generations.
- With $\Lambda = 1$ TeV, constraints are set on coupling coefficients for both detector-level and particle-level fits.

Coupling coefficient	Operator
$c_{lq}^{(3)}$	$(\bar{l}\sigma^i\gamma^\mu l)(\bar{q}\sigma^i\gamma^\mu q)$
$c_{lq}^{(1)}$	$(\bar{l}\gamma^\mu l)(\bar{q}\gamma^\mu q)$
c_{lu}	$(\bar{l}\gamma^\mu l)(\bar{u}\gamma^\mu u)$
c_{ld}	$(\bar{l}\gamma^\mu l)(\bar{d}\gamma^\mu d)$
$c_{q\tau}$	$(\bar{\tau}\gamma^\mu\tau)(\bar{q}\gamma^\mu q)$
$c_{\tau u}$	$(\bar{\tau}\gamma^\mu\tau)(\bar{u}\gamma^\mu u)$
$c_{\tau d}$	$(\bar{\tau}\gamma^\mu\tau)(\bar{d}\gamma^\mu d)$
c_{ll}	$(\bar{l}\gamma^\mu l)(\bar{l}\gamma^\mu l)$
$c_{Hl}^{(3)}$	$(H^\dagger i\overleftrightarrow{D}^i_\mu H)(\bar{l}\sigma^i\gamma^\mu l)$
$c_{Hl}^{(1)}$	$(H^\dagger i\overleftrightarrow{D}_\mu H)(\bar{l}\gamma^\mu l)$
$c_{H\tau}$	$(H^\dagger i\overleftrightarrow{D}_\mu H)(\bar{\tau}\gamma^\mu\tau)$
$c_{\tau W}$	$(\bar{l}\sigma^{\mu\nu}\tau)\sigma^i H W^i_{\mu\nu}$
$c_{\tau B}$	$(\bar{l}\sigma^{\mu\nu}\tau)H B_{\mu\nu}$
$c_{\tau Z}$	$(\bar{l}\sigma^{\mu\nu}\tau)\sigma^i H(c_W\sigma^i W^i_{\mu\nu} + s_W B_{\mu\nu})$
$c_{\tau\gamma}$	$(\bar{l}\sigma^{\mu\nu}\tau)\sigma^i H(-s_W\sigma^i W^i_{\mu\nu} + c_W B_{\mu\nu})$

Relevant SMEFT coupling coefficients to this measurement

Interpretation

CONTUR

- **Contur**: a BSM interpretation tool that uses existing particle-level SM predictions and measurements with preserved **Rivet** routines.
  - **Under the assumption of large statistics, Confidence Levels are calculated from test statistics:**

$$t_{\mu} = \left(\vec{x} - \mu \cdot \vec{s} - \vec{b}\right)^{T} \cdot \mathrm{Cov}^{-1} \cdot \left(\vec{x} - \mu \cdot \vec{s} - \vec{b}\right)$$

s = signal, b = SM background, μ = signal-strength parameter

- Recently added function: **Spey** to get limits and best-fit values on the μ
  - The function is currently under development - the Contur team is actively working on getting this function fully implementable for all analyses with preserved Rivet routines.

- Offered an insight on the c_i limits that can be extracted from particle-level results.

- Contur results provided tighter constraints than detector-level fits, which were done with coarser bins.

Interpretation

Particle-level stand-alone fitting

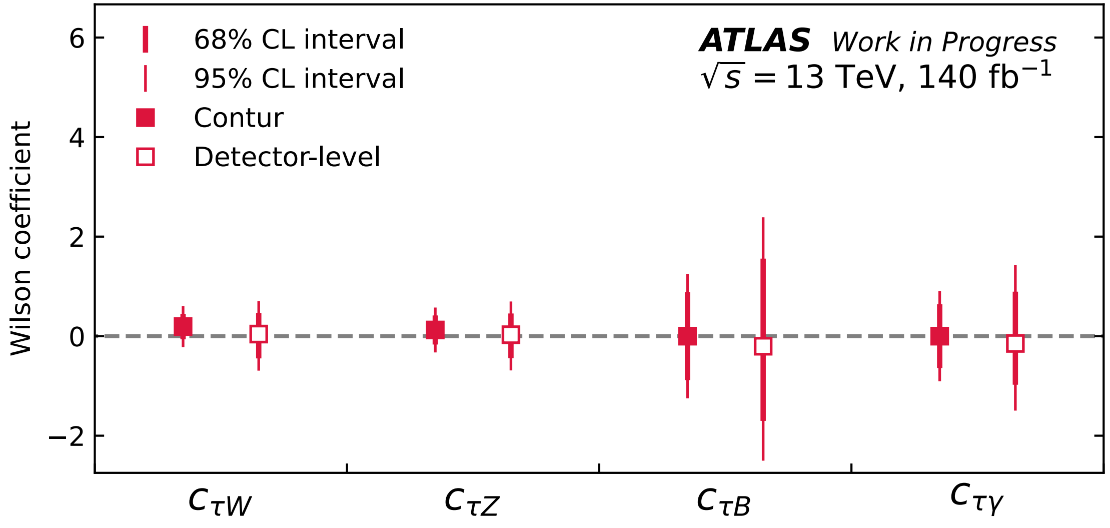

- Current limitations on Contur on μ fitting:
  - ➢ The combined (Interference+Pure BSM) histogram is used, so $\boldsymbol{\mu}$ is not directly comparable to c_i .
  - ➢ c_i scaling on covariance matrices.

- The initial Contur limits (left plot) were obtained using either Interference-only or BSM-only event files as a conservative approach.

- A dedicated stand-alone script was also written to:
  - ➢ Carry out a χ^2 fit on a signal strength parameter μ, that scales linearly for the BSM-SM interference terms and quadratically for the BSM-only terms.

Interpretation

SM Effective Field Theory (SMEFT)

- Overall: Particle-level is giving more constrained results
  - ➢ higher sensitivity towards the higher masses, where unfolded measurements have finer bins.

- Particle-level and Contur results differences due to limitations discussed previously.
  - ➢ To be resolved in future Contur developments.

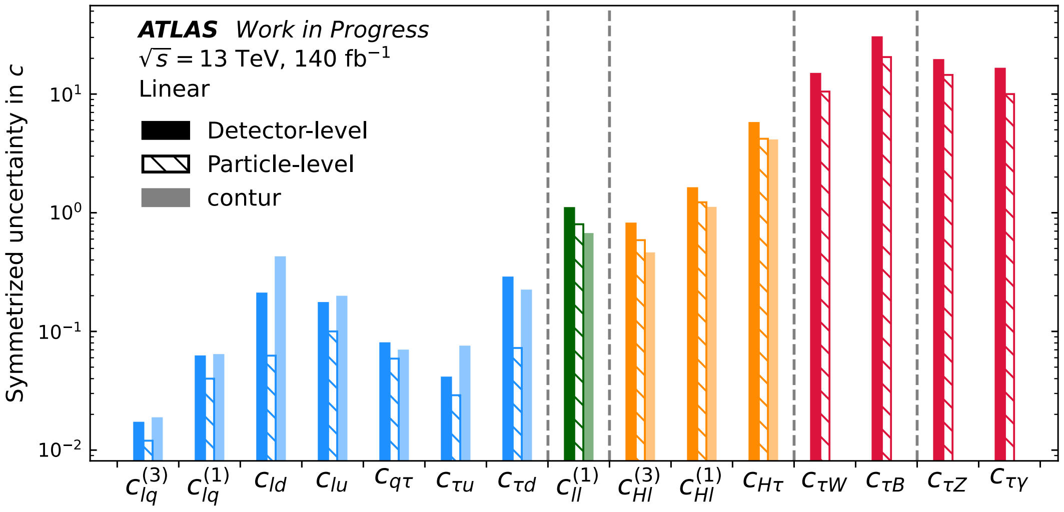

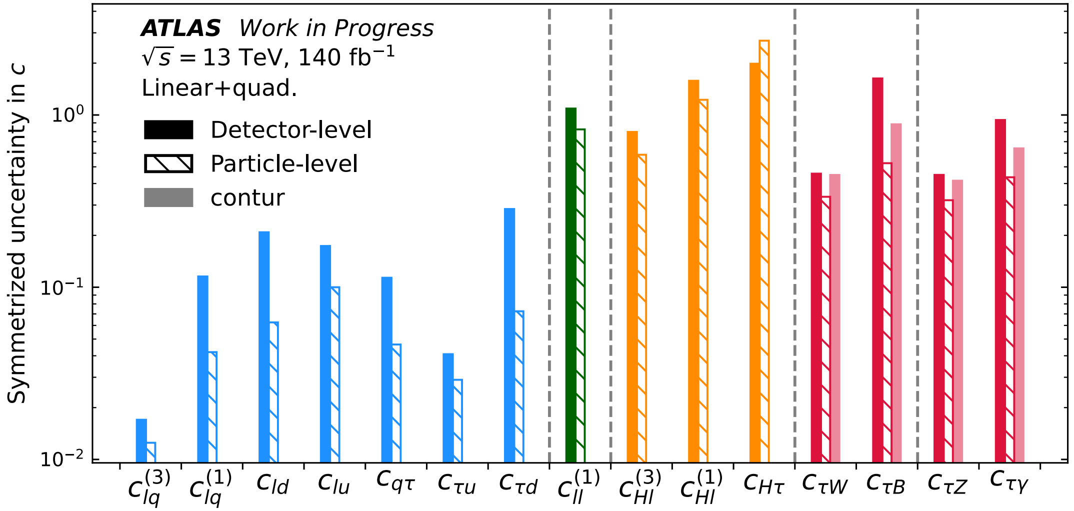

Fitted coefficients BSM-SM interference terms (LH) plot and BSM+Interference terms (RH) plot

Interpretation

SM Effective Field Theory (SMEFT)

- The coefficient $c_{\tau\gamma}$ is a linear combination of 'top' operators that contributes to the anomalous magnetic moment a_τ of the τ lepton, and to the electric dipole moment d_τ if $c_{\tau\gamma}$ is complex

https://arxiv.org/pdf/2307.14133

$$a_\tau = \frac{2\sqrt{2} m_\tau v}{e} \frac{\mathrm{Re}(c_{\tau\gamma})}{\Lambda^2} \qquad d_\tau = -\sqrt{2} v \frac{\mathrm{Im}(c_{\tau\gamma})}{\Lambda^2}.$$

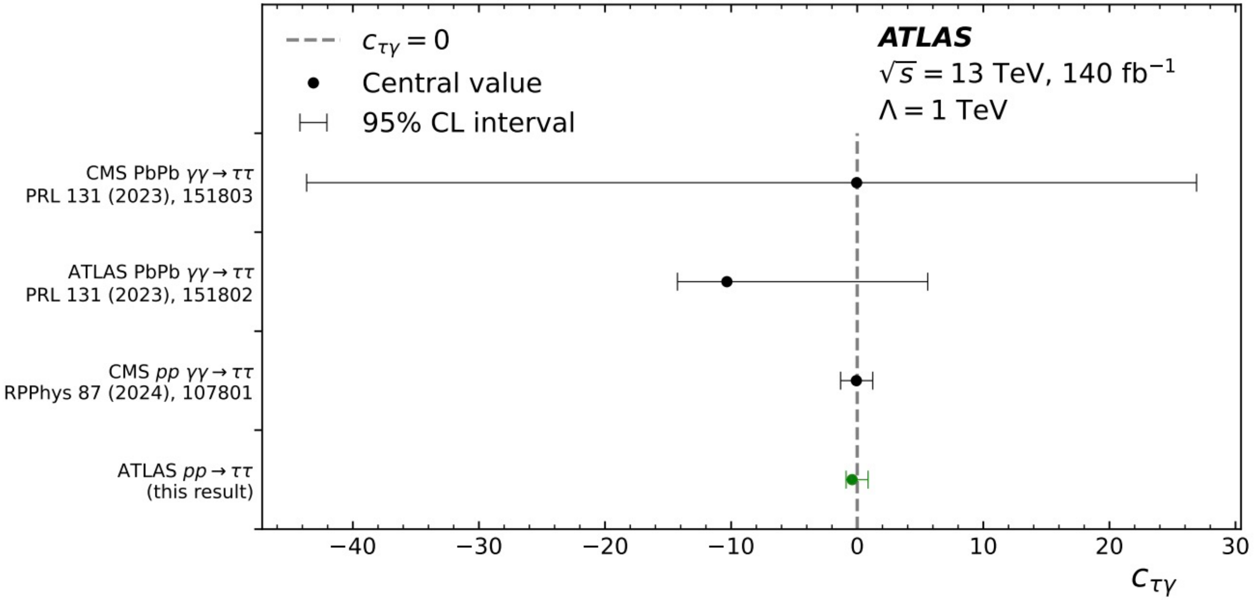

- However, a_τ is defined for on-shell photons with $q^2 = 0$, whereas we rely on off-shell photon exchange, so comparison is restricted to $c_{\tau\gamma}$
- From Particle-level fits: $c_{\tau\gamma} = -0.400^{+0.630}_{-0.240}$, ~ a factor of seven smaller than the ATLAS measurement in ultra-peripheral lead-lead collisions
- Competitive with the CMS analysis of $\gamma\gamma \to \tau\tau$ limits in $p\,p$ collisions

Conclusion

- The first unfolded differential measurement of inclusive $\tau\tau$ production has been performed using 140 fb^{-1} Full Run-2 ATLAS 13TeV pp collision data.

- The measurement is consistent with the Standard Model predictions, fitting MEPS@NLO SM prediction with unfolded data gives a p-value of 0.78.

- SMEFT coupling coefficients involving first two generation quarks are constrained by performing a χ^2 fit using the unfolded measurement.
    - Particle-level fit gives: $c_{\tau\gamma} = -0.400^{+0.630}_{-0.240}$, a factor of seven smaller than the ATLAS, competitive with the 2024 CMS $\gamma\gamma \rightarrow \tau\tau$ limits

Thank you

Backup

Motivation

- Di-tau mass spectrum is sensitive to new physics that has enhanced couplings to 3rd generation fermions. E.g. Heavy Z' Bosons, Leptoquarks.
  - Possible explanations to [3.2σ deviation in $R_D/R_D{}^*$] (R_D related to $b \rightarrow c\tau\nu$ rates).

- EFT Interpretation: constrains several Wilson Coefficients.

- The first 13TeV measurement of the inclusive $\tau\bar{\tau}$ fiducial cross-section as a function of the invariant mass.

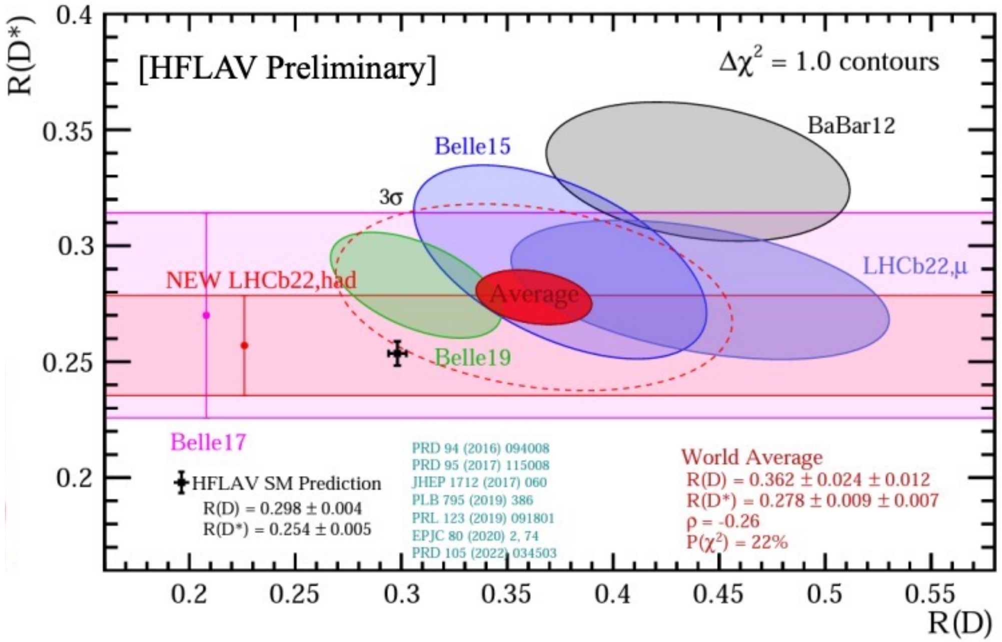

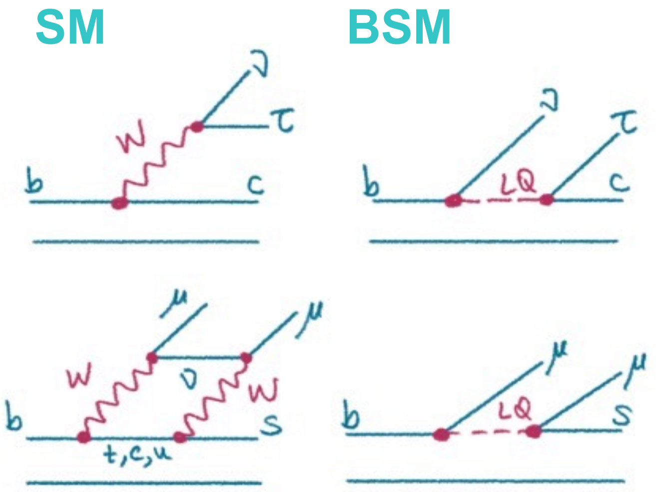

Object Selections

- τ_{had}:
  - Identified using Tight RNN identification working point
  - eBDT used to reduce electrons faking taus, required to pass Loose Working Point (WP).
  - $|\eta|$< 2.47 and lead p_T> 90 GeV, sub-lead p_T > 60GeV after τ_{had} energy scale (TES) corrections
- e & μ:
  - Pass the MEDIUM identification working point .
  - FCHighPtCaloOnly isolation for electrons and FCLoose isolation for muons;.
  - p_T > 7 GeV. $|\eta|$< 2.47 for electrons and $|\eta|$< 2.5 for muons.
- *Jets*: Standard anti-kT particle flow jets with R = 0.4
- *b-jets*: DL1r b-tagger with b-jet identification efficiency 77% at operating point

Standard ATLAS algorithms and calibrations are used for physics object reconstruction in each case

Particle-level Object Selections

particle-level objects are selected using criteria reflecting the detector-level requirements as closely as possible

- τ_{had}: $|\eta|$< 2.47, excluding 1.37<$|\eta|$<1.52 ; lead p_T>90 GeV, sub-lead p_T > 60GeV
- e: $|\eta|$< 2.47, excluding 1.37<$|\eta|$<1.52 ; dressed p_T > 7 GeV
- μ: $|\eta|$< 2.5 for muons, excluding 1.37<$|\eta|$<1.52 ; dressed p_T > 7 GeV ; Prompt
- *Jets:* Anti-k_T with R = 0.4; built from stable particles; p_T>20GeV ; $|y| < 4.4$
- *b-jets*: contain a weakly-decaying, ghost-associated $b-$hadrons with p_T> 5 GeV.

Fiducial Event Selection:

- $\tau_{had}\tau_{had}$: $\geq$ 2 fiducial τ_{had} in an event, $m_{\tau\tau}^{vis}$ is built using 2 highest- p_T $\boldsymbol{\tau_{had}}$
- $e\tau_{had}$ / $\mu\tau_{had}$: == 1 fiducial τ_{had} and ≥ 1 e/μ .
- Events with fewer than one accepted particle-level τ_{had} are treated as non-fiducial.

Fake Estimate

- One of the major sources of backgrounds comes from fake-taus
- This is estimated using the data-driven **Universal Fake Factors (FF) method**
- We define the anti-ID region as taus in the signal region but with an opposite RNN score cut.

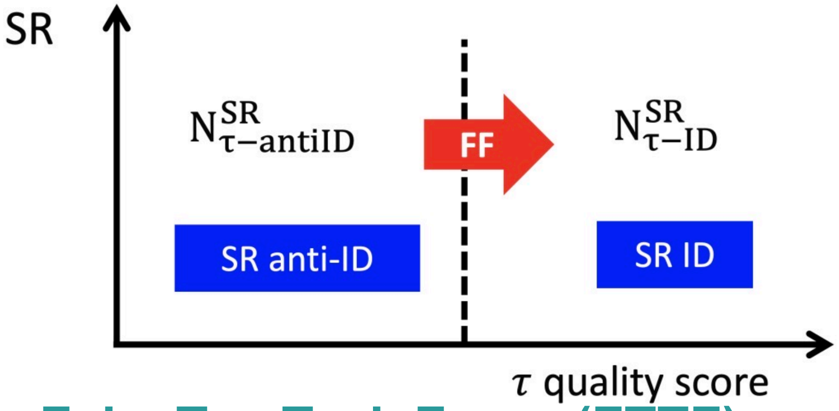

$$FF = \frac{N^{CR}_{ID}}{N^{CR}_{anti-ID}}$$

$$N^{SR}_{ID} = N^{SR}_{antiID} \times FF$$

The **Fake Tau Task Force (FTTF)** provides the anti-ID to ID transfer factor (fake factor) for three types of jets:

- Quark-enriched jets from a $Z \rightarrow \mu\mu$ data sample.
- Gluon-enriched jets from a multijet data sample with high JVT score.
- Pileup-enriched jets from a multijet data sample with low JVT score.

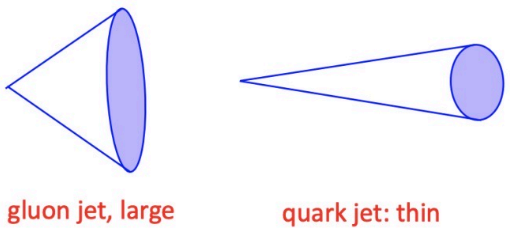

Unfolding

- Detector effects are unfolded using standard iterative Bayesian methods with **two iterations**:
  - ➢ This is optimized with Bias significance studies across 1-4 iterations
  - ➢ Bias is defined as $\text{Bias} = \frac{U_i - P_i}{P_i}$ where U_i = Unfolded yield and P_i = Particle-level yield.
  - ➢ Bias significance is defined as:
    - $\text{Bias}_{\text{sig}} = \frac{Bias}{\Delta P_{i,stats}}$

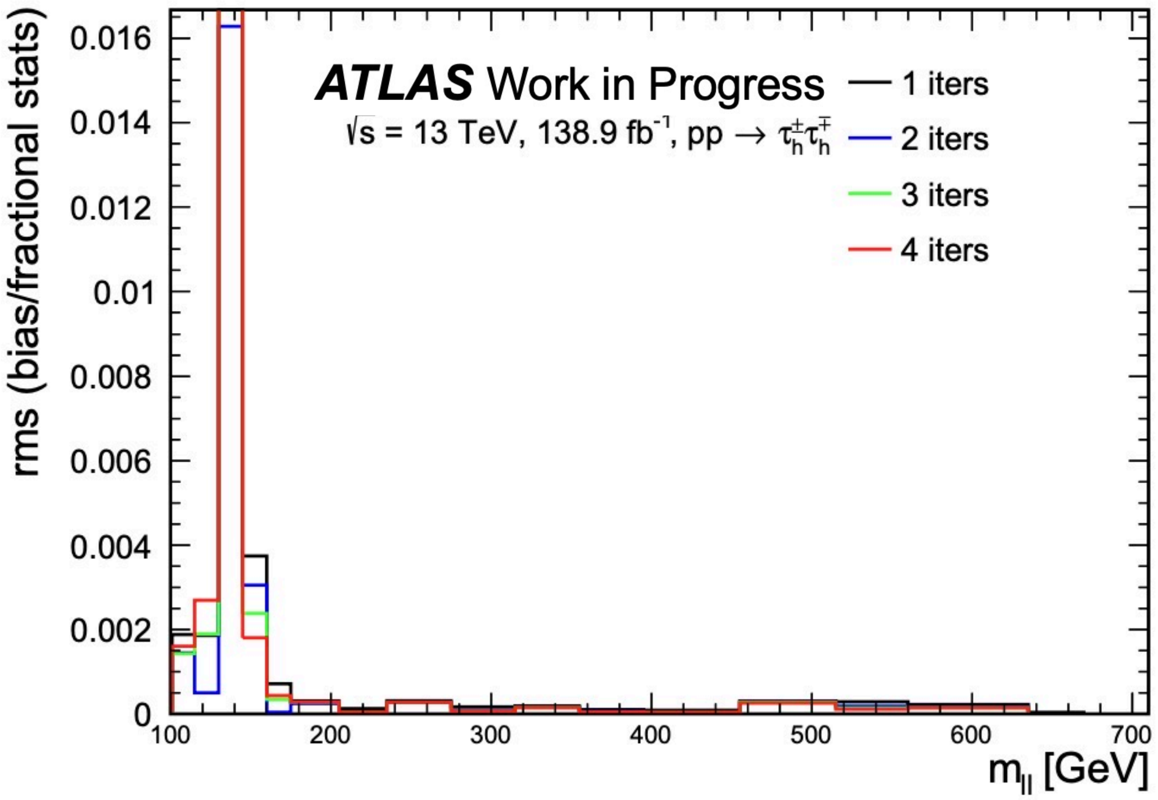

Unfolding

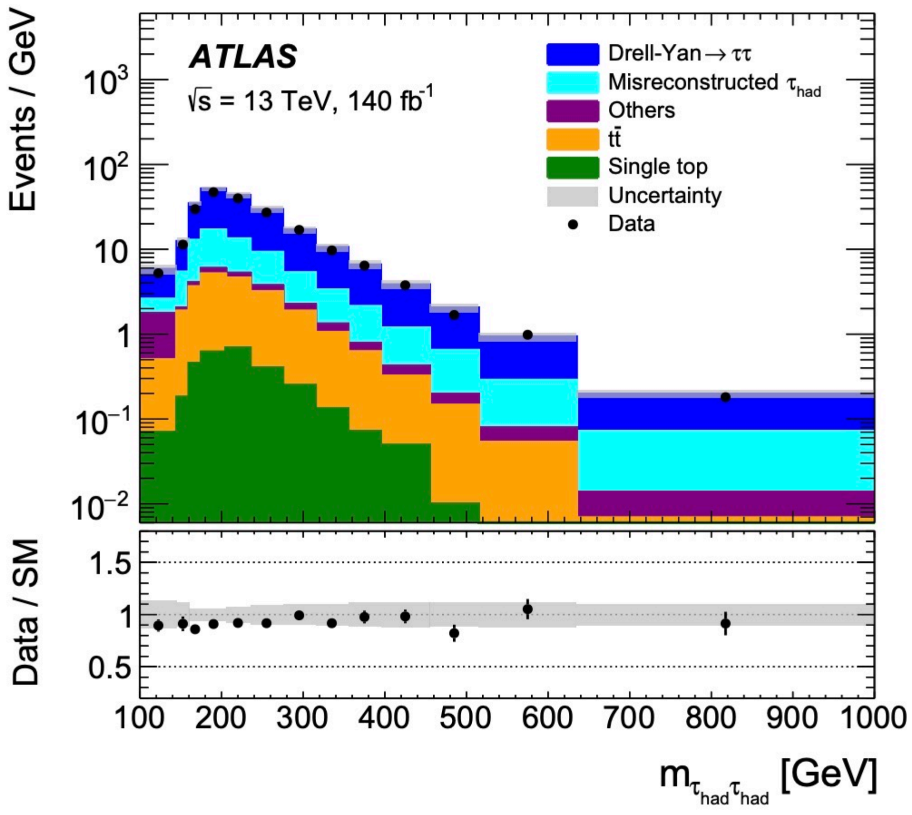

The $\tau_{had}\,\tau_{had}$ visible invariant mass in region of the measurement, before background subtraction and correction for detector effect

Unfolding Cross-checks Overview

- **Trivial Closure**: sanity check for closure between unfolded reco-level MC and truth-level MC
- **Statistically fluctuated Asimov sample test**
- **BSM Signal Injection tests:**
  - Add vector_LQ_UFO model BSM signal onto SM Reco-level MC, then do statistical fluctuation
  - Scale the BSM signal up to get 3σ discrepancy compared to SM Reco-level MC
- **Constant Scale Factor (SF) = 1.2** applied to all bins on $m_{\tau\tau}$ distribution
- **Linear reweighting function on $m_{\tau\tau}$**, with a lower value at lower mass end $SF = A \times m_{\tau\tau}$, where A is a constant
  - SF ranged from 1 to 1.2
  - SF ranged from 1.1 to 1.5
- **Process composition reweighting:**
  - Scale up $Z \rightarrow \tau\tau$ Samples by a Scale Factor of 1.1
  - Scale up $t\bar{t}$ Samples by a Scale Factor of 1.1
- **Shifting $m_{\tau\tau}$ to higher masses** on event-by-event basis
  - Shifting by 1GeV
  - Shifting by 2GeV
- **Reweighting using bin-to-bin scale factors from comparing p_T^{ll} Reco-level distribution to data**

Cross-checks only

- **Data-driven Closure test (Post Unblinding)**: Reweight to data to estimate **unfolding uncertainty**

Added with other uncertainties

Unfolding: Cross-checks

Trivial Closure check (Sanity Check)

- Reco-level MC is used as input for unfolding (labelled as unfolded pseudodata)
- Compared to MC-truth (labelled Standard Model)
- Perfect Closure observed

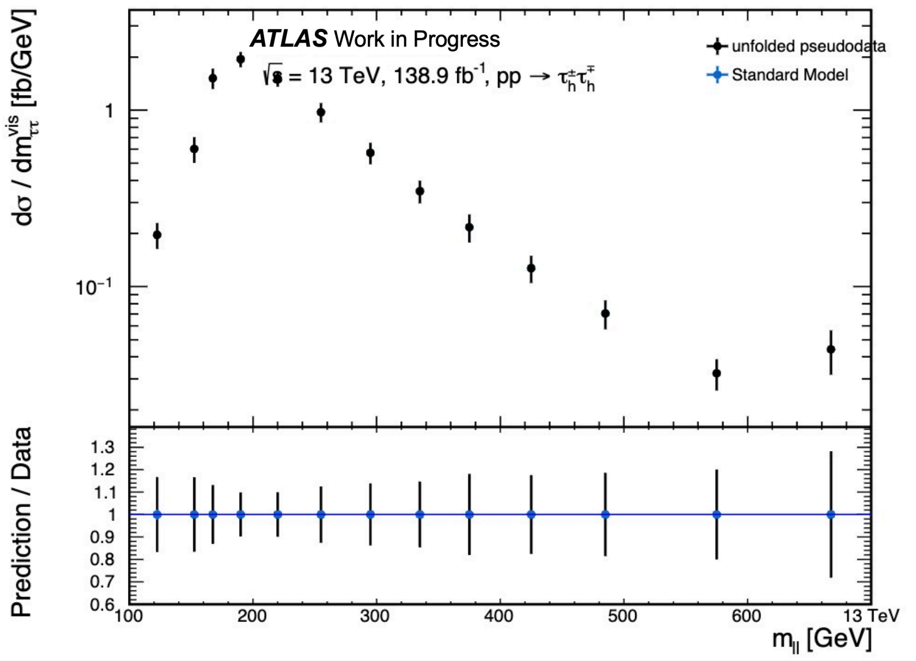

Closure check with Statistical fluctuations

- Gaussian fluctuated Reco-level MC is used as input for unfolding (unfolded pseudodata)
- Compared to MC-truth (Standard Model)
- Good Closure observed

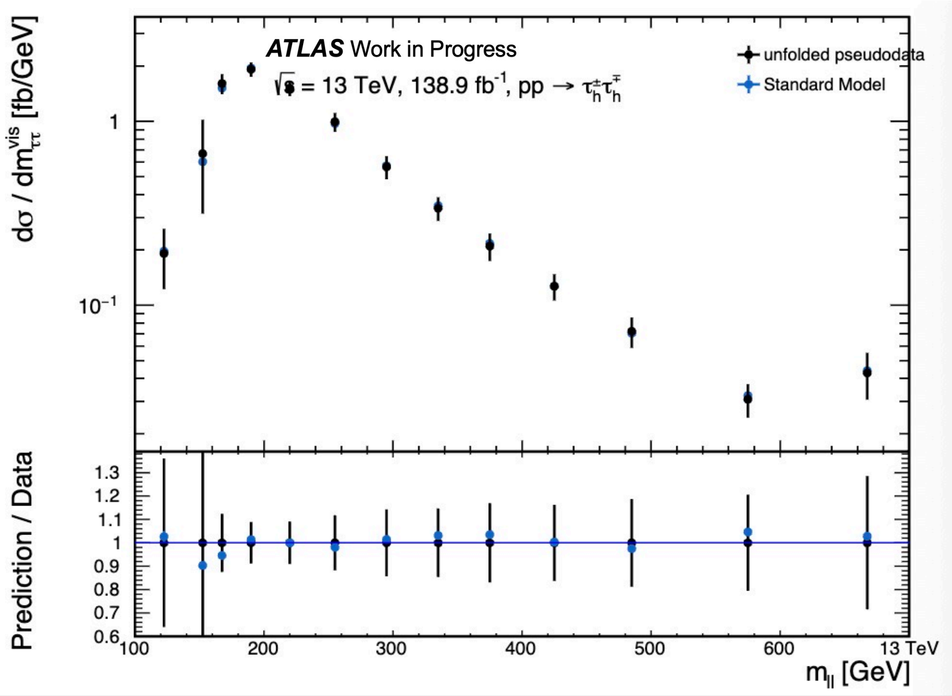

Unfolding: Cross-Checks

BSM Injection

- Pseudodata is created with BSM signal added to the SM MC then fluctuated.
- The BSM signal used here is generated using the vector_LQ_UFO model with MadGraph
  - ➢ The leptoquark coupling to third generation left-handed fermion fields is turned on and the mass of the leptoquark is set to be 1.5 TeV
- This checks if the nominal response matrix manages to recover the potential BSM signal in the data

BSM Truth-level injection

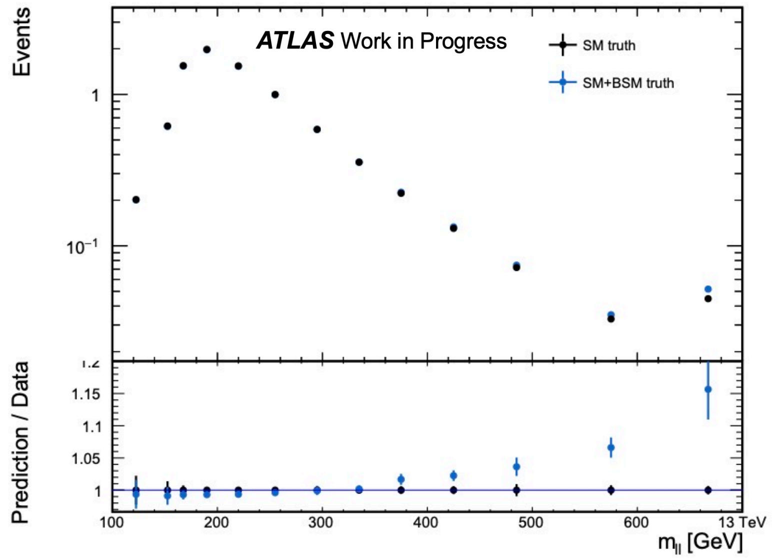

unfolded SM+BSM Reco v.s Truth SM+BSM

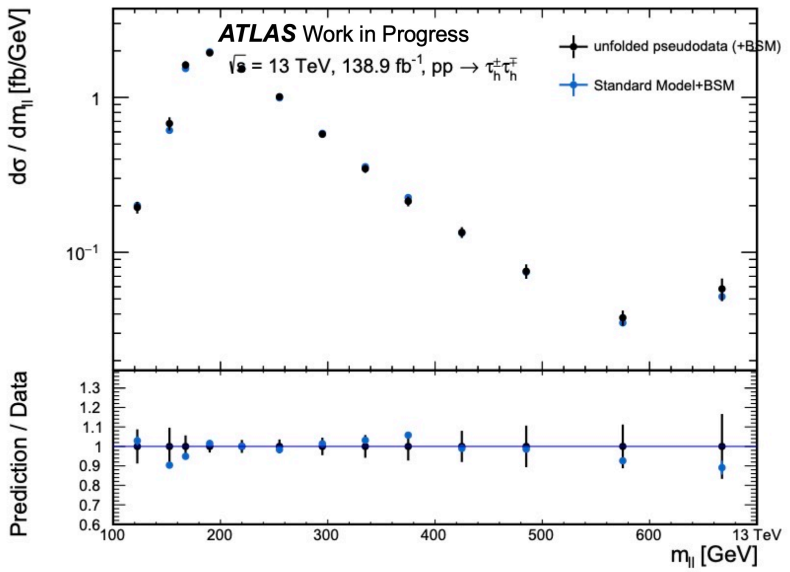

Unfolding: Cross-Checks

$m_{\tau\tau}$ spectrum shift (2GeV)

- $m_{\tau\tau}$ is shifted 2GeV higher on an event-by-event basis
- Ratio between the shifted spectrum and the original spectrum is taken as the scaling factor and then applied to SM Reco-level MC.
- This is then fluctuated to give pseudodata
- Good Closure is seen between unfolded pseudodata and shifted Truth MC.

SM Truth vs Shifted Truth

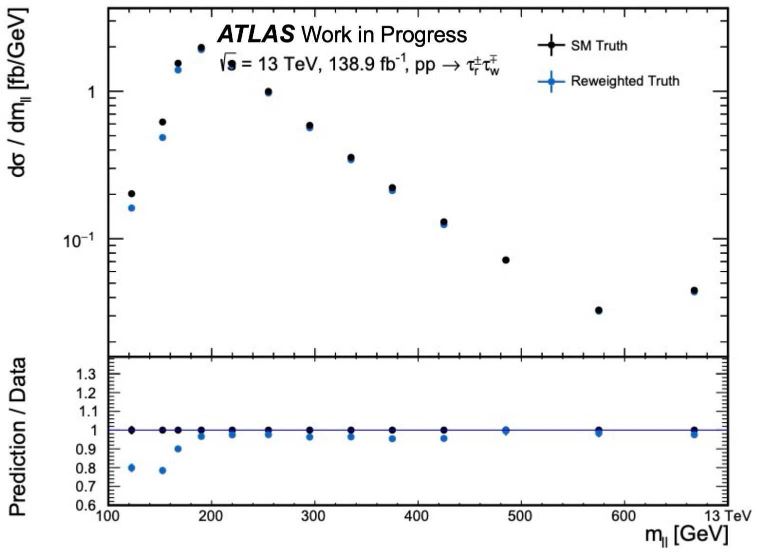

unfolded pseudodata vs Shifted Truth

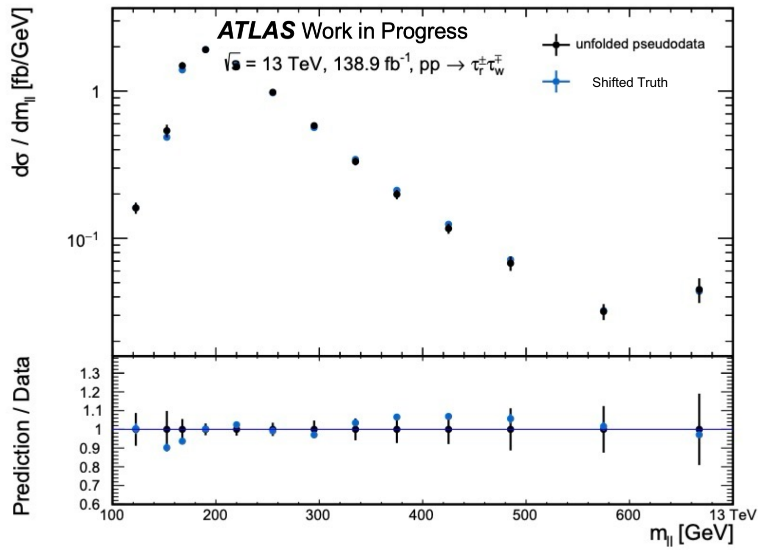

Unfolding: Cross-Checks

p_T^{ll} Reweighting

- p_T^{ll} Reco-level distribution is compared to data, and the ratios between the two are taken as bin-to-bin scale factors.
- These scale factors are applied to Truth-level generation on event-by-event basis.
- The reco-level generation with the reweighting applied is then taken as pseudodata for unfolding.
- Good Closure is seen between unfolded pseudodata and shifted Truth MC.

Data vs SM Reco p_T^{ll} distribution

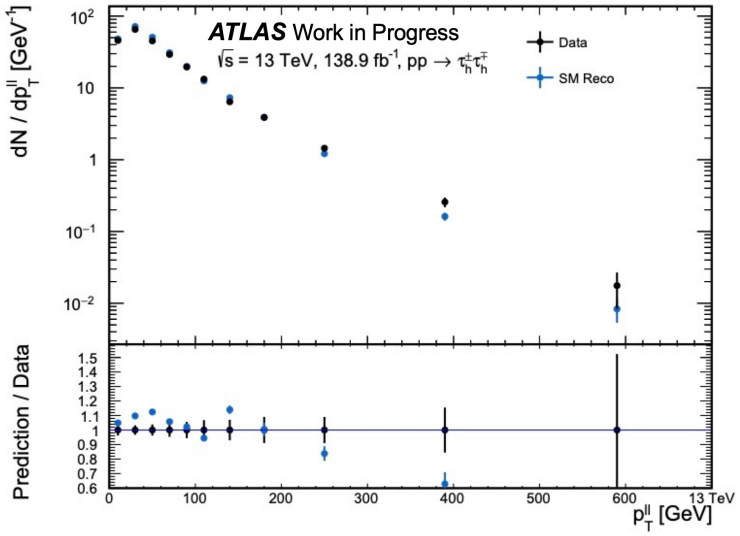

unfolded pseudodata vs SM prediction m_{ll} distribution

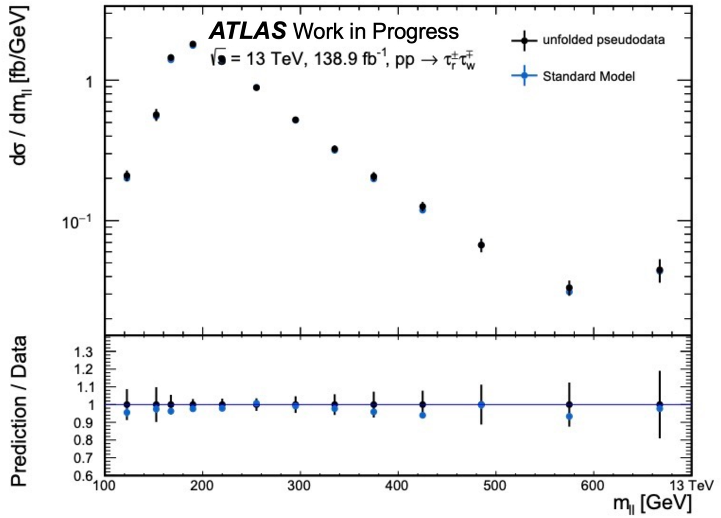

Uncertainties

Uncertainties on unfolded data

- **Experimental Uncertainties:**
  - ➢ 260 recommended uncertainties in total.
  - ➢ Impact of each one is checked, and pruned if the size is <10% of the statistical uncertainty.
  - ➢ 69 non-negligible systematic uncertainties after pruning.

- **Modelling uncertainty:**
  - ➢ **Two-Point Systematics:** Powheg+Pythia8 is compared with Powheg+Herwig7 if available, otherwise, Powheg+Pythia8 vs Sherpa 2.2.11 to assess generator uncertainties
  - ➢ **Data-driven Closure test (Post Unblinding)**: Reweight to data to estimate **unfolding uncertainty**

Before Pruning

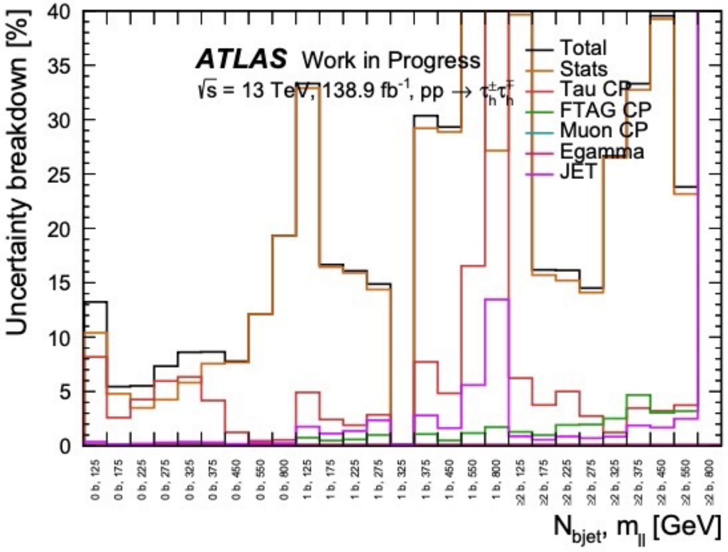

After Pruning

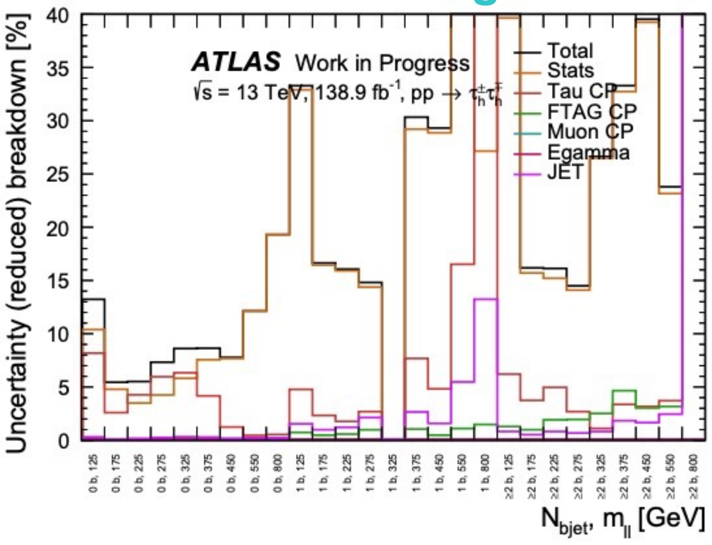

Interpretation

SM Effective Field Theory (SMEFT)

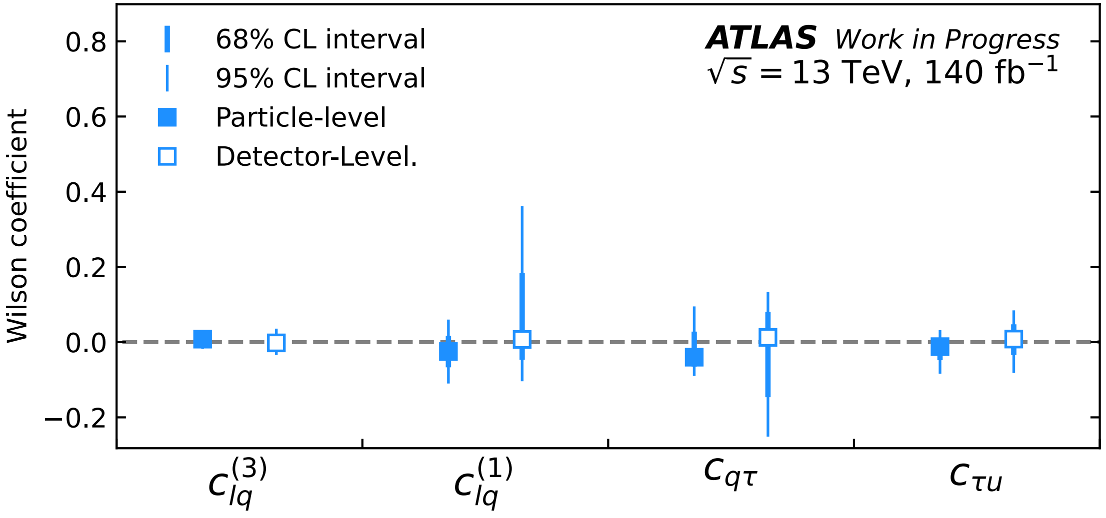

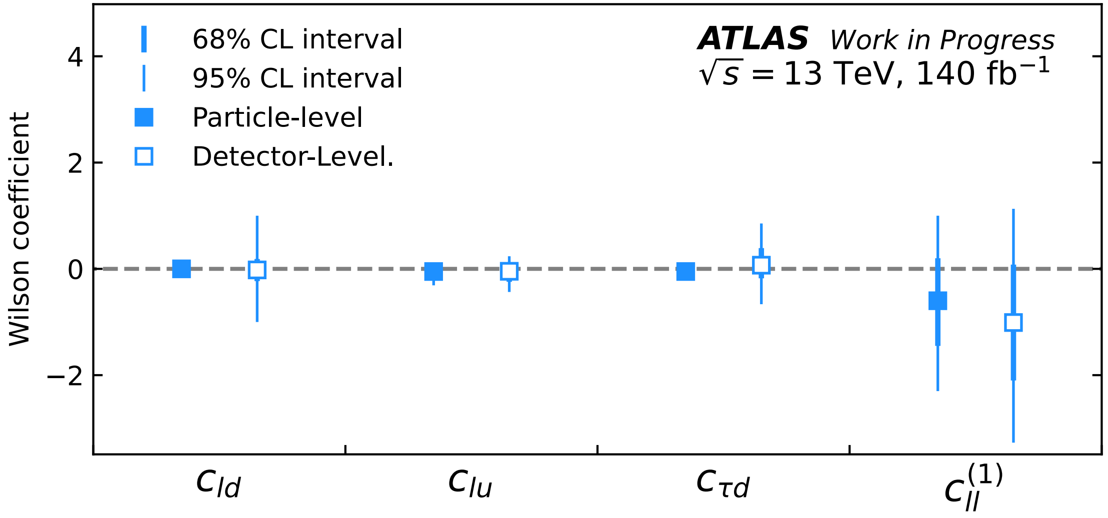

Interpretation

SM Effective Field Theory (SMEFT)